Innovare Academic Sciences

International Journal of Pharmacy and Pharmaceutical Sciences

ISSN- 0975-1491 Vol 7, Issue 12, 2015

Original Article

DESIGN, *IN-SILICO* DOCKING AND PREDICTIVE ADME PROPERTIES OF NOVEL PYRAZOLINE DERIVATIVES WITH SELECTIVE HUMAN MAO INHIBITORY ACTIVITY

VISHNU NAYAK BADAVATH*, BARIJ NAYAN SINHA, VENKATESAN JAYAPRAKASH

Department of Pharmaceutical Sciences and Technology, Birla Institute of Technology, Mesra, Ranchi 835215, Jharkhand, India
Email: vishnu.niper@gmail.com

Received: 25 Sep 2015 Revised and Accepted: 02 Nov 2015

ABSTRACT

Objectives: Curcumin, a known hMAO-A (human Monoamine oxidase-A) inhibitor from *Curcuma longa* has never been recognized for this property due to its poor permeability and extensive metabolism. Thus, the main objective of this study is to incorporate structural features of Curcumin in the pyrazoline scaffold as an attempt to get potent, selective hMAO-isoform inhibitors with improved permeability.

Methods: A series of twelve novel 4, 4'-(4, 5-dihydro-1H-pyrazole-3,5-diyl)bis(2-methoxyphenol) derivatives (1-12) were designed based on the structure of Curcumin. All the designed compounds were evaluated for their hMAO inhibitory activity by *in-silico* docking studies (Autodock4.20). The both isomers (R-and S-isomer) are considered for simulation approach to understand the effect of chirality and other structural features that determine the potency and selectivity. In order to judge the pharmacokinetic behavior, all the derivatives were evaluated for their *in-silico* ADME properties by using Qik Prop v 3.0.

Results: The results of the present study showed that all the designed compounds were found to be potent and selective hMAO-isoform inhibitors, and exhibited lead like properties from the calculated ADME parameters. Curcumin was taken as a standard for comparison to judge any improvement in permeability.

Conclusion: The design strategy adopted has predicted improved potency, selective towards hMAO-isoform and permeability characteristics in comparison with Curcumin.

Keywords: Pyrazoline, hMAO inhibitors, Molecular docking simulation, Autodock4.20, Pharmacokinetic parameters, Schrodinger LLC, Structure-activity relationship.

INTRODUCTION

Monoamine oxidases are FAD (Flavin adenine dinucleotide) containing enzymes located on the mitochondrial outer membrane exists in two different isoforms, MAO-A and MAO-B. They metabolize dietary amines, neurotransmitters, are identified by the difference in their specificity towards their substrate and their selective inhibitors [1, 2]. Serotonin, adrenaline, and noradrenaline are preferably metabolized by MAO-A [3], while *β*-phenylethylamine and benzylamine by MAO-B [4]. Tyramine, dopamine, and some other important amines are common substrates for both the MAO-isoforms [5]. MAO-inhibitors introduced earlier were abandoned from clinical practice mainly due to their adverse effects; these adverse effects were mainly attributed to non-selective inhibition of isoforms. In the past decade, the interest in MAO inhibitors got renewed due to the fact that isoform-selective inhibitors, that are reversible, are showing potential therapeutic utility in the treatment of depression (MAO-A selective) and neurodegenerative disorders (MAO-B selective) [6–8].

Earlier few researcher synthesized pyrazoline derivatives and stated that the calculated (Ki value) obtained from the molecular docking studies (by AutoDock) concerning the hMAO inhibitory activities of the compounds were found to be in a good agreement with the experimental Ki value [9,10]. Thus, the present study *in-silico* docking has been performed to understand the interactions of Curcumin-based pyrazoline derivatives (1-12), which are crucial for their hMAO-isoform inhibitory activity. I*n-silico* ADME parameters have also been performed by QikProp v 3.0.

Rationale of designing potent and selective hMAO-isoform inhibitors

Curcumin, a natural compound with proven MAO inhibitory and antidepressant activity [11–16]. As curcumin was having poor bioavailability [17], it is never recognized as a good antidepressant due to its poor permeability and bioavailability. The half-life ($t_{1/2}$) of Curcumin in phosphate buffered saline (PBS) at pH 7.2 was less than 10 min due to extensive metabolism [18]. In humans, Moclobemide (MOC) is rapidly and almost completely absorbed and totally metabolized by the liver [19], about 44 percent of the drug is lost due to the first pass effect through the liver [20]. The elimination half-life is around 2 h [21]. Selegiline (SEL) has a low oral bioavailability, which increases to moderate when ingested together with a high-fat meal, the molecule being fat soluble [22]. Selegiline oral bioavailability is drastically increased in females taking oral contraceptives (10-to 20-fold) [23]. This could lead to lose of MAO-B selectivity in favor of an MAO-A selectivity, which in turn would make patients susceptible to the usual risks of non-selective hMAO-inhibitors such as tyramine-induced hypertensive [23].

The novel pyrazoline derivatives (1-12) have been designed by utilizing the structural features in Curcumin. We design chalcone that resembles aryl-α,β-unsaturated carbonyl portion of Curcumin but by reversing the position of the double bond and the carbonyl group, then chalcone was cyclized to provide a series of novel pyrazoline derivatives (1-12) table 1, fig. 1.

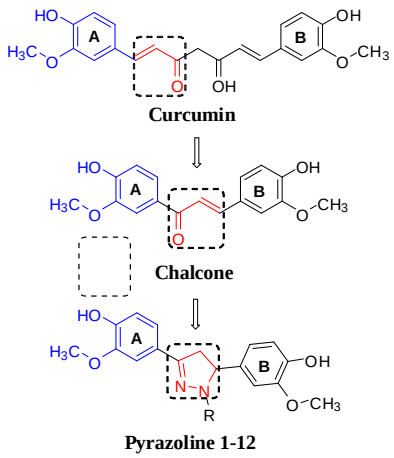

Table 1: Structure of designed novel pyrazolines (1-12)

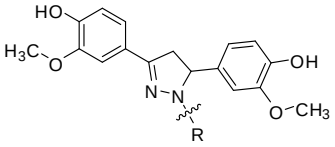

Compound	R	Compound	R
1	H	7	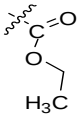
2	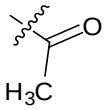	8	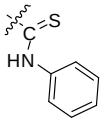
3	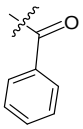	9	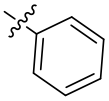
4	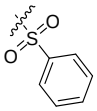	10	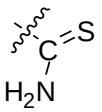
5	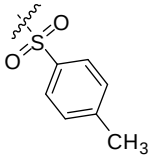	11	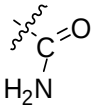
6	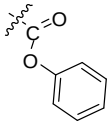	12	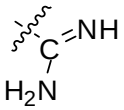

MATERIALS AND METHODS

Molecular docking studies were carried on RHEL-5.0 Operating system installed on Dell Precision workstation with Intel core 2 quad processor and 8 GB RAM by using AutoDock4.2 (The Sripps Research Institute) [24].

Molecular docking simulation procedures

In order to understand the interaction at the molecular level, compounds 1-12 were docked with X-ray crystal structure of hMAO-A (PDB: 2BXR) and hMAO-B (PDB: 2BYB) using AutoDock4.2 docking protocol reported earlier [25-30].

Ligand preparation

Ligand structures were drawn using build panel and prepared using Ligprep module implemented Maestro-8.4 (Schrodinger LLC). Energy minimization is carried out using OPLS 2005 force field. Structures were saved in PDB format for AutoDock compatibility. MGL Tools-1.5.6 (The Sripps Research Institute) was used to convert ligand. pdb files to the ligand. PDB qt files.

Protein preparation

X-ray crystal structure of hMAO-A (PDB ID: 2BXR) and hMAO-B (PDB ID: 2BYB) were downloaded from protein data bank (www. rcsb. org). Protein preparation wizard Maestro-8.4 (Schrodinger LLC) was used to prepare protein. Water molecules were removed from the protein, FAD was reconstructed, side chains were optimized for hydrogen bonding and finally energy minimized using OPLS 2001 force field. The protein was then saved in the PDB format. Using MGL Tools-1.5.6 nonpolar hydrogens were merged, assigned AD4.2 type, Gasteiger charges and finally saved in protein. PDB qt format.

Docking protocol

For docking, grid parameter file (. gpf) and docking parameter files (. dpf) were written using MGL Tools-1.5.6. Receptor grids were generated using 60×60×60 Grid points in xyz with a grid spacing of 0.375Å. Grid box was centered on N5 atom of FAD. Map types were generated using Autogrid 4.2. Docking was carried out with following parameters with a number of runs: 50, population size: 150, the number of evaluations: 2,500,000 and number of generations: 27,000, using Autodock 4.2.

Autodock run

Both protein and ligand were selected as a. PDB qt file from "docking". Autodock was run for each ligand. Docking output was obtained as a. dlg format. Analysis of docking results was done using MGL Tools-1.5.6. A Top scoring molecule in the largest cluster was analyzed for its interaction with the protein.

ADME parameters prediction

ADME parameters were calculated using QikProp v 3.0 tools of Schrodinger software [31]. Qik Prop provides ranges for comparing an exact molecule's properties with those of 95% of known drugs. QikProp also flags 30 types of reactive functional groups that may cause false positives in high throughput screening assays. It also evaluates the suitability of derivatives based on Lipinski's rule of five [32-35], which is essential to ensure drug-like pharmacokinetic profile while using rational drug design. All the analogs were neutralized before being used by Qik Prop v3.0.

RESULTS AND DISCUSSION

Molecular docking simulation

Molecular docking simulation was carried out to understand the effect of chirality and other structural features that determine the

potency and selectivity of designed novel pyrazoline derivatives (1-12). The 5C carbon of pyrazoline is chiral in nature and two isomers are possible. In the presented work, we considered both the R-and S-isomer to check the effect of chirality on potency and selectivity towards hMAO-isoforms. From the simulation results it seems the substituent's at 1*N*position of pyrazoline has some effect in determining the potency of the isomers (R-isomer and S-isomer). Except compound 1 was found to be hMAO-B selective, when there is no substitution at 1*N* position of pyrazoline, while other compounds (2-12) having substituent's at 1*N* position of pyrazoline increase in bulkiness and shifts selectivity towards MAO-A isoform with increase in potency too according to the Inhibitory constant (Ki) values obtained by docking analysis. Ki values are represented in table 2. According to the calculated Ki values, compound 8 exhibited the highest hMAO-A inhibitory activity, with higher SI than the standard drug Moclobemide SI. R-isomers of compounds (2, 6-8 and 10-12) were found to perform better than S-isomer, while in case of compounds (3, 5 and 9) S-isomer were found to perform better than R-isomer. Compound 4 R-and S-isomers were found to be equipotent towards hMAO-isoforms. For comparison ki value obtained by Autodock studies, the averages of R-and S-isomers were calculated for each isoform, and their isomer potency and selectivity index were calculated for better understanding. SI was calculated as K_i (MAO-A)/Ki(MAO-B). Selectivity towards MAO-A increases as the corresponding SI decreases while selectivity towards MAO-B isoform increases as the corresponding SI increases. Curcumin, SEL and MOC selectivity index was considered instead of selectivity MAO-A_{rac}/MAO-B_{rac}. (table 2). In order to understand the factors that contribute towards the selectivity and potency of the docked complexes of potent compounds (R-and S-isomers) were studied for their orientation and interactions in active site cavity of hMAO-isoforms were discussed below which sheds a light on the key structural features responsible for their potency and selectivity.

Orientation of compounds (1-12) in active site of hMAO-A

R-isomers compound 10 ring A at 3rd position of pyrazoline towards pocket 2 (lined by Ile180, Ile335, Leu337, Met350 and Phe352). Ring B at the 5th position of pyrazoline orient towards pocket 3 (lined by Gly74, Arg206, Ile207, Phe208, Glu216 and Trp441) and 1*N*-substitution of pyrazoline towards pocket 1 (aromatic cage lined by FAD, Tyr407, and Tyr444). All other compounds ring B towards the aromatic cage, ring A towards pocket 3, 1*N*-substituent's towards pocket 2.

Orientation of compounds (1-12) in active site of hMAO-A

S-isomers Compound 1 orient in such a way that ring A towards pocket 3, ring B towards pocket 2, this will keep the aromatic cage empty. Compound (2-6 and 9-12) having 1*N* substituents fills the aromatic cage while rings A and ring B orient same as compound 1. Compound 7 and 8 having similar orientation ring A towards pocket 3 (same as compound 1-6 and 9-12) but ring B towards pocket 1 and 1*N*-substituents towards pocket 2, and these may be the reason that 1*N*-substituted pyrazolines exhibit selectivity towards hMAO-A isoform. Compound 8 having the bulkier substitution at 1*N* position than compound 7 these may be the reason why compound 8 having better Ki value than compound 7.

Interaction of compound (3) with hMAO-A

S-isomer Phenyl ring (Ring A) at 3rd position of pyrazoline towards pocket 3, ring A establishes π-π interaction with Trp441 and with FAD, moreover ring A hydroxy oxygen forms a hydrogen bond with the oxygen of Pro72. Phenyl ring (Ring B) at the 5th position of pyrazoline occupy pocket 2, and establishes π-π interaction with Tyr69. This places the substitution at 1*N* position to orient towards pocket 1, establishes π-π interaction with Tyr69, this may be the reason that S-isomer shows better (Ki value), potency and selectivity than R-isomer fig. 2.

Interaction of compound (3) with hMAO-A

R-isomer Phenyl ring (Ring A) at 3rd position of pyrazoline occupy pocket 3, and ring A establishes π-π interaction with Trp441. Phenyl ring (Ring B) at the 5th position of pyrazoline occupy pocket 1. The substitution at 1*N* position of pyrazoline orient towards pocket 2 fig. 3.

Interaction of compound (8) with hMAO-A

R-isomer Phenyl ring (Ring A) at 3rd position of pyrazoline occupy pocket 3, and establishes π-π interaction with Trp441and Phe352. Phenyl ring (Ring B) at the 5th position of pyrazoline towards pocket 1 and establishes π-π interaction with Phe352, moreover ring B-hydroxy oxygen forms a hydrogen bond with the oxygen of Tyr407. The substitution at 1*N* position of pyrazoline orient towards pocket 2 fig. 4.

Orientation of compounds (1-12) in active site of hMAO-B

R-isomers compound 11 ring A towards aromatic cage (formed by FAD, Tyr435, and Tyr398). Ring B and 1*N*-substituents of pyrazolines towards hydrophobic pocket (characterized by LEU171, TYR326, PHE168, ILE198, and ILE199). All other compounds ring B and 1*N*-substitution towards the aromatic cage, while ring A towards the hydrophobic cage.

Orientation of compounds (1-12) in active site of hMAO-B

S-isomers compound 8 ring A and ring B towards aromatic cage (formed by FAD, Tyr435, and Tyr398), and 1*N*-substitutituents towards the hydrophobic pocket, all other compounds ring B and 1*N*-substitution towards aromatic cage and ring A towards the hydrophobic cage.

Interaction of compound (1) with hMAO-B

R-isomer Phenyl ring (Ring B) at the 5rd position of pyrazoline orient towards the aromatic cage, the hydroxy group of ring B established H-bonding interaction with 5N of FAD, this interaction is mainly stabilized by the strongπ-π interaction between Bring of the compound 1and the FAD. Phenyl ring (Ring A) at the 3th position of pyrazoline keeps in the hydrophobic pocket and anchoring from their face of FAD with a distance of 3.564 Å, moreover establishes π-π interaction with Tyr435 fig. 5.

Table 2: Calculated K_i values corresponding to the inhibition of hMAO-isoforms by novel pyrazoline derivatives 1-12

Compound	MAO-A Calc. Ki (µM)		Isomer potency (R/S)	Racemic potency MAO-A_{rac} =[(R+S)/2]	MAO-B Calc. Ki (µM)		Isomer potency (R/S)	Racemic potency MAO-B_{rac} =[(R+S)/2]	Selectivity MAO-A_{rac}/MAO-B_{rac}	MAO Selectivity
	R	S			R	S				
1	2.20	5.36	0.41	3.78	0.296	0.493	0.600406	0.789	4.79	MAO-B
2	1.87	4.83	0.38	3.35	247.51	3.32	74.5512	250.83	0.01	MAO-A
3	61.66	0.035	1761.71	30.84	-	258.92	-	-	-	MAO-A
4	0.151	0.151	1	0.15	35350	-	-	-	-	MAO-A
5	0.376	0.196	1.91	0.28	203310	-	-	-	-	MAO-A
6	0.090	0.192	0.46	0.14	266.12	143000	0.001	143266.1	$9x10^{-7}$	MAO-A
7	0.750	2.85	0.263	1.8	9220	3.09	2983.81	9223.09	0.000195	MAO-A
8	0.281	0.483	0.58	0.38	-	-	-	-	-	MAO-A
9	0.441	0.238	1.85	0.33	9910	44.09	224.76	9954.09	0.00003	MAO-A
10	0.423	1.20	0.35	0.81	6.89	0.925	7.44	7.815	0.10	MAO-A
11	1.71	6.72	0.25	4.21	216.73	10.65	20.35	227.38	0.01	MAO-A
12	9.13	20.27	0.45	14.7	72910	186.57	390.79	73096.57	0.000201	MAO-A
Curcumin	0.602		-	-	16.40		-	-	0.036	MAO-A
MOC	7.91		-	-	12.13		-	-	0.652	MAO-A
SEL	78.26		-	-	93.62		-	-	0.835	MAO-B

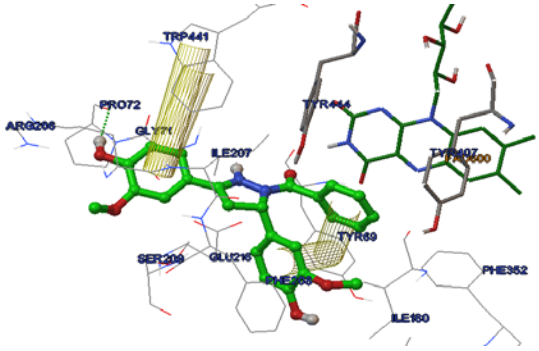

Fig. 2: Interaction of S-enantiomer of Compound (3) with hMAO-A (PDB: 2BXR) active site, H-bonds are shown as green dots and π-π interaction as yellow cylinders

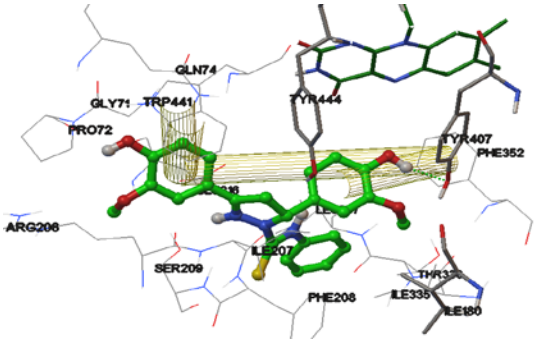

Fig. 4: Interaction of R-enantiomer of Compound (8) with hMAO-A (PDB: 2BXR) active site, H-bonds are shown as green dots and π-π interaction as yellow cylinders

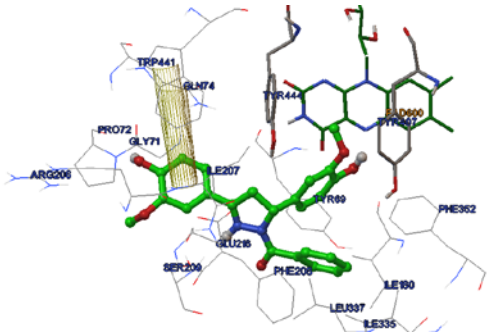

Fig. 3: Interaction of R-enantiomer of Compound (3) with hMAO-A (PDB: 2BXR) active site, H-bonds are shown as green dots and π-π interaction as yellow cylinders

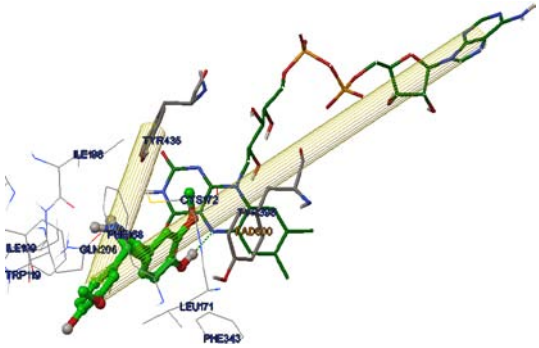

Fig. 5: Interaction of R-enantiomer of Compound (1) with hMAO-B (PDB: 2BYB) active site, H-bonds are shown as green dots and π-π interaction as yellow cylinders

Table 3: Predicted ADME parameters of novel designed pyrazoline derivative using QikProp

Compound	Mol. Formula	Mol. Weight	Log Po/w	Log S	Log BB	PMDCK	Human oral absorption (%)	Lipinski's violations
1 (R)	$C_{17}H_{18}N_2O_4$	314.34	2.467	-4.166	-0.931	263.777	90.564	0
1 (S)			2.477	-4.238	-0.958	255.304	90.387	0
2 (R)	$C_{19}H_{20}N_2O_5$	356.37	2.669	-4.694	-1.065	204.091	89.899	0
2 (S)			2.669	-4.694	-1.065	203.993	89.894	0
3 (R)	$C_{24}H_{22}N_2O_5$	418.44	3.832	-5.476	-1.044	247.981	100	0
3 (S)			3.83	-5.471	-1.044	247.944	100	0
4 (R)	$C_{23}H_{22}N_2O_6S$	454.50	3.374	-5.279	-1.309	169.404	92.62	0
4 (S)			2.789	-4.182	-1.218	142.414	87.882	0
5 (R)	$C_{24}H_{24}N_2O_6S$	468.52	3.666	-5.814	-1.354	169.137	94.319	0
5 (S)			3.059	-4.52	-1.222	145.353	89.606	0
6 (R)	$C_{24}H_{22}N_2O_6$	434.44	4.048	-6.078	-1.092	274.421	100	0
6 (S)			4.049	-6.08	-1.091	274.542	100	0
7 (R)	$C_{20}H_{22}N_2O_6$	386.40	3.27	-5.38	-1.179	205.149	93.455	0
7 (S)			3.27	-5.382	-1.18	204.793	93.445	0
8 (R)	$C_{24}H_{23}N_3O_4S$	449.52	4.733	-6.648	-0.629	1172.325	100	0
8 (S)			4.678	-6.428	-0.592	1201.794	100	0
9 (R)	$C_{23}H_{22}N_2O_4$	390.43	4.879	-6.379	-0.617	653.791	100	0
9 (S)			4.88	-6.379	-0.617	653.51	100	0
10 (R)	$C_{18}H_{19}N_3O_4S$	373.43	2.699	-4.91	-0.847	575.814	91.096	0
10 (S)			2.699	-4.91	-0.848	575.465	91.093	0
11 (R)	$C_{18}H_{19}N_3O_5$	357.36	1.415	-3.063	-1.526	67.614	68.59	0
11 (S)			1.416	-3.065	-1.527	67.571	68.591	0
12 (R)	$C_{18}H_{20}N_4O_4$	356.38	2.042	-4.069	-1.673	61.088	77.555	0
12 (S)			2.042	-4.068	-1.672	61.086	77.555	0
Curcumin	$C_{21}H_{20}O_6$	368.38	2.96	-4.349	-1.897	128.192	88.259	0
MOC	$C_{13}H_{17}ClN_2O_2$	268.739	1.829	-2.233	0.378	978.137	89.028	0
SEL	$C_{13}H_{17}N$	187.281	3.093	-2.09	0.646	1396.996	100	0

ADME parameterss

All the designed pyrazoline derivatives (1-12) R-and S-isomer were subjected for their predictive ADME parameters with their R and S-isomers, for physical descriptors and pharmaceutically significant properties of pyrazoline derivatives using QikProp v3.0 tool of Schrodinger software, among which major descriptors reported here are required for predicting the drug-like properties of molecules.

These properties are:

1. Molecular weight (Mol. Wt.) (150-650)

2. Octanol/water partition coefficient (Log Po/w) (-2-6.5)

3. Aqueous solubility (QPlogS) (−6.5-0.5)

4. Apparent Madin–Darby canine kidney (MDCK) cell permeability (QPPMDCK) (<25 poor,>500 great)

5. Brain/blood partition coefficient (QPlogBB) (−3.0-1.2)

6. Percent human oral absorption (≥80% is high, ≤25% is poor).

All the novel designed pyrazoline derivatives (1-12) (R-and S-isomers) showed significant drug-like characteristics based on Lipinski's rule of 5. table 3. The designed pyrazoline derivatives follow the three properties of Lipinski rule of five (Mol. Wt.)<650, (logPo/w) between-2 to 6.5 and (QPlogS)7. (QPlogBB) parameter indicated the ability of the drug to pass through the blood-brain barrier which is mandatory for selective hMAO-B inhibition. The QPPMDCK predicted apparent MDCK cell permeability in nm/s. MDCK cells are considered to be a good mimic for the blood-brain barrier and higher the value of QPPMDCK, higher the cell permeability. All designed compounds showed ADME parameters in an acceptable range.

CONCLUSION

All the designed pyrazoline derivatives (1-12) were found to be potent and selective hMAO-isoform inhibitory activity than Curcumin. The results obtained by docking studies could be utilized for the development of novel pyrazoline derivatives with potent and selective hMAO-isoform inhibitory activity. The result of ADME parameters showed that all the designed pyrazolines exhibit lead like properties. The design strategy adopted has significantly improved the permeability characteristics in comparison with Curcumin.

ACKNOWLEDGEMENT

Author acknowledge to Birla Institute of Technology for providing financial support as a prestigious Institute Fellowship.

CONFLICT OF INTERESTS

Declared None

REFERENCES

1. Youdim MBH, Collins GGS, Sandler M, Jones ABB, Pare CMB, Nicholson WJ. Biological sciences: human brain monoamine oxidase: multiple forms and selective inhibitors. Nature 1972;236:225–8.
2. Collins GGS, Sandler M, Williams ED, Youdim MBH. Multiple forms of human brain mitochondrial monoamine oxidase. Nature 1970;225:817–20.
3. Johnson JP. Some observations upon a new inhibitor of monoamine oxidase in brain tissue. Biochem Pharmacol 1968;17:1285–97.
4. Knoll J, Magyar K. Some puzzling pharmacological effects of monoamine oxidase inhibitors. Adv Biochem Psychopharmacol 1972;5:393-408.
5. O Carroll AM, Fowler CJ, Phillips JP, Tobbia I, Tipton KF. The deamination of dopamine by human brain monoamine oxidase-Specificity for the two enzyme forms in seven brain regions. Naunyn-Schmiedeberg's Arch Pharmacol 1983;322:198–202.
6. Da Prada M, Keller HH, Kettler R. Comparison of the new MAO-A inhibitors moclobemide, brofaromine and toloxatone with tranylcypromine in an animal experiment: significance for clinical practice. Psychiatr Prax 1989;16(Suppl 1):18–24.
7. Lavian G, Finberg JP, Youdim MB. The advent of a new generation of monoamine oxidase inhibitor antidepressants: pharmacologic studies with moclobemide and brofaromine. Clin Neuropharmacol 1993;16(Suppl 2):S1–7.
8. Youdim MBH, Weinstock M. Therapeutic applications of selective and non-selective inhibitors of monoamine oxidase A and B that do not cause significant tyramine potentiation. Neurotoxicology 2004;25:243–50.
9. Mishra N, Sasmal D. Development of selective and reversible pyrazoline based MAO-B inhibitors: virtual screening, synthesis and biological evaluation. Bioorg. Med Chem Lett 2011;21:1969–73.
10. Mathew B, Suresh J, Anbazhagan S, Elizabeth Mathew G. Pyrazoline: a promising scaffold for the inhibition of monoamine oxidase. Cent Nerv Syst Agents Med Chem 2013;13:195–206.
11. Xu Y, Ku BS, Yao HY, Lin YH, Ma X, Zhang YH, *et al.* Antidepressant effects of curcumin in the forced swim test and olfactory bulbectomy models of depression in rats. Pharmacol Biochem Behav 2005;82:200–6.
12. Kulkarni SK, Bhutani MK, Bishnoi M. Antidepressant activity of curcumin: Involvement of serotonin and dopamine system. Psychopharmacology 2008;201:435–42.
13. Rajeswari A, Sabesan M. Inhibition of monoamine oxidase-B by the polyphenolic compound, curcumin and its metabolite tetrahydrocurcumin, in a model of Parkinson's disease induced by MPTP neurodegeneration in mice. Inflammopharmacology 2008;16:96–9.
14. Zhang L, Luo J, Zhang M, Yao W, Ma X, Yu SY. Effects of curcumin on chronic, unpredictable, mild, stress-induced depressive-like behaviour and structural plasticity in the lateral amygdala of rats. Int J Neuropsychopharmacol 2014;17:793–806.
15. Wang R, Xu Y, Wu HL, Li YB, Li YH, Guo JB, *et al.* The antidepressant effects of curcumin in the forced swimming test involve 5-HT1 and 5-HT2 receptors. Eur J Pharmacol 2008;578:43–50.
16. Xu Y, Ku BS, Yao HY, Lin YH, Ma X, Zhang YH, *et al.* The effects of curcumin on depressive-like behaviors in mice. Eur J Pharmacol 2005;518:40–6.
17. Tonnesen HH, Masson M, Loftsson T. Studies of curcumin and curcuminoids. XXVII. Cyclodextrin complexation: Solubility, chemical and photochemical stability. Int J Pharm 2002;244:127–35.
18. Wang. YJ, Pan MH, Cheng AL, Lin LI, Ho YS, Hsieh CY, *et al.* Stability of curcumin in buffer solutions and characterization of its degradation products. J Pharm Biomed Anal 1997;15:1867–76.
19. Mayersohn M, Guentert TW. Clinical pharmacokinetics of the monoamine oxidase-a inhibitor moclobemide. Clin Pharmacokinet 1995;29:292–332.
20. Raaflaub J, Haefelfinger P, Trautmann KH. Single-dose pharmacokinetics of the mao-inhibitor moclobemide in man. Arzneimittelforschung 1984;34:80–2.
21. Nair NPV, Ahmed SK, Ng Ying Kin NMK. Biochemistry and pharmacology of reversible inhibitors of MAO-A agents: focus on moclobemide. J Neuropsychiatry Clin Neurosci 1993;18:214–25.
22. Barrett JS, Szego P, Rohatagi S, Morales RJ, DeWitt KE, Rajewski G, *et al*. Absorption and presystemic metabolism of selegiline hydrochloride at different regions in the gastrointestinal tract in healthy males. Pharm Res 1996;13:1535–40.
23. Laine K, Anttila M, Helminen A, Karnani H, Huupponen R. Dose linearity study of selegiline pharmacokinetics after oral administration: evidence for strong drug interaction with female sex steroids. Br J Clin Pharmacol 1999;47:249–54.
24. Morris GM, Huey R, Lindstrom W, Sanner MF, Belew RK, Goodsell DS, *et al.* AutoDock4 and AutoDockTools4:Automated docking with selective receptor flexibility. J Comput Chem 2009;30:2785–91.
25. Vishnu Nayak B, Ciftci-Yabanoglu S, Soumendranath B, Ajay K. T, Barij N Sinha, Ucar, G, Mahmoud E S S, Venkatesan J. Monoamine oxidase inhibitory activity of 2-aryl-4H-chromen-4-ones. Bioorg Chem 2015; 58: 72–80.
26. Vishnu Nayak B, Ciftci-Yabanoglu S, Jadav SS, Jagrat M, Sinha BN, Ucar G, *et al.* Monoamine oxidase inhibitory activity of 3,5-biaryl-4,5-dihydro-1H-pyrazole-1-carboxylate derivatives. Eur J Med Chem 2013;69:762–7.
27. Sahoo A, Yabanoglu S, Sinha BN, Ucar G, Basu A, Jayaprakash V. Towards development of selective and reversible pyrazoline based MAO-inhibitors: Synthesis, biological evaluation and docking studies. Bioorganic Med Chem Lett 2010;20:132–6.
28. Jagrat M, Behera J, Yabanoglu S, Ercan A, Ucar G, Sinha BN, *et al.* Pyrazoline based MAO inhibitors: synthesis, biological evaluation and SAR studies. Bioorg Med Chem Lett 2011;21:4296–300.
29. Chimenti F, Bolasco A, Manna F, Secci D, Chimenti P, Befani O, *et al.* Synthesis and selective inhibitory activity of 1-acetyl-3, 5-

diphenyl-4, 5-dihydro-(1 H)-pyrazole derivatives against monoamine oxidase. J Med Chem 2004;47:2071–4.

30. Chimenti F, Fioravanti R, Bolasco A, Manna F, Chimenti P, Secci D, *et al.* Synthesis, molecular modeling studies and selective inhibitory activity against MAO of N1-propanoyl-3,5-diphenyl-4,5-dihydro-(1H)-pyrazole derivatives. Eur J Med Chem 2008;43:2262-7.
31. Schrodinger LLC. Maestro 8.5 user manual; 2008.
32. Debnath B, Ganguly S. Molecular docking studies and ADME prediction of novel Isatin analogs as Hiv-1-Rt inhibitors with broad spectrum chemotherapeutic properties. Asian J Pharm Clin Res 2014;7:186-94.
33. Ganguly S, Debnath B. Molecular docking studies and ADME prediction of novel Isatin analogs with potent anti-EGFR activity. Med Chem 2014;4:558–68.
34. Lipinski CA, Lombardo F, Dominy BW, Feeney PJ. Experimental and computational approaches to estimate solubility and permeability in drug discovery and development settings. Adv Drug Delivery Rev 1997;23:3-25.
35. Lipinski CA, Lombardo F, Dominy BW, Feeney PJ. Experimental and computational approaches to estimate solubility and permeability in drug discovery and development settings. Adv Drug Delivery Rev 2001;46:3-26.